Characterization and degradation study of chitosan-siloxane hybrid microspheres synthesized using a microfluidic approach

doi: info:doi/10.1016/j.msec.2017.08.035

Characterization and degradation study of chitosan-siloxane hybrid microspheres synthesized using a microfluidic approach

Susana Cruz-Neves[1], Yuki Shirosaki[2*], Toshiki Miyazaki[1], Satoshi Hayakawa[3]

1 Graduate School of Life Science and Systems Engineering, Kyushu Institute of Technology, 2-4 Hibikino, Wakamatsu-ku, Kitakyushu, Fukuoka, 808-0196, Japan

2 Graduate School of Engineering, Kyushu Institute of Technology, 1-1 Sensui-cho, Tobata-ku, Kitakyushu, Fukuoka, 804-8550, Japan

3 Graduate School of Natural Science and Engineering, Okayama University, 3-1-1 Tsushima, Kita-ku, Okayama, 700-8530, Japan

Corresponding author

Yuki Shirosaki

Graduate School of Engineering, Kyushu Institute of Technology, 1-1 Sensui-cho, Tobata-ku, Kitakyushu, Fukuoka, 804-8550, Japan

Tel/Fax: +81-93-884-3302

e-mail: *yukis@che.kyutech.ac.jp

Abstract

Chitosan microspheres can address challenges associated with poor bioavailability or unsustained drug release when used as drug delivery systems thanks to their mucoadhesiveness, which allows the drug dosage to be retained in the gastrointestinal track for extended periods. Chitosan-3-glycidoxypropyltrimethoxysilane-β-glycerophosphate (chitosan-GPTMS-β-GP) hybrid microspheres were synthetized through sol-gel processing using a microfluidic approach. Microspheres with uniform spherical shapes and sizes of approximately 650 μm were obtained. The microstructures of the microspheres consisted of four different siloxane structures. The degradation behaviors of the hybrid microspheres were examined under acidic pH conditions mimicking those found in the gastrointestinal track. Microspheres with different GPTMS molar ratios were incubated under several pH conditions for 2 weeks. The microspheres incubated at pH 7.4 extended the lowest weight loss (27%-32%), whereas those incubated at pH 1.7 and pH 5.4 showed greater weight losses of 43-59% and 69-77%, respectively. The inhibition of the degradation at low pH was dependent on the siloxane network in the chitosan matrix. Phosphate was mostly released in early stages,

and the released amount of silicon was dependent on the composition. GPTMS was released with a chitosan chain via the hydrolysis of a chitosan molecule. The pelargonidin was incorporated in the microspheres and the slow releasing was observed at acidic condition. The resistance of these hybrid microspheres to low-pH conditions for longer than a full digestion cycle is promising for gastrointestinal drug delivery applications.

Keywords: Chitosan-siloxane hybrid, Microspheres, Microfluidic system, Degradation

1. Introduction

Biodegradable microspheres have presented several advantages compared with conventional delivery systems. For instance, they offer a more sustained and controlled release of drugs over time, thereby reducing the need for multiple doses and allowing the release of insoluble drugs [1,2]. Moreover, both synthetic and natural polymers are normally cleaved into biocompatible byproducts, resulting in no bodily harm [3]. Even though microspheres are small, they have large surface area to volume ratios [1,2]. The synthesis of microspheres with good size uniformity has been reported when using a microfluidic approach [4,5]. This method is simple and has the advantage of using small solution volumes.

Organic-inorganic hybrids that involve natural biodegradable polymers such as chitosan, are studied by researchers in the form of scaffolds, films, hydrogels and spherical particles. In particular, the organic-inorganic hybrid hydrogels are suitable candidate for drug carrier controlled the releasing [6-8]. Chitosan is a natural polymer that consists of polysaccharide chains. The biocompatible, bioresorbable, mucoadhesive, non-toxic and non-antigenic [9-11] properties of chitosan make it a

suitable candidate for medical applications. Additionally, chitosan-mediated systems can considerably improve the bioavailability across the epithelial layer of the oral cavity [12] and gastrointestinal track [13]. However, this polymer lacks mechanical endurance and a controlled degradation rate [1]. To overcome these disadvantages, non-toxic crosslinking agents are required. Shirosaki *et al.* assessed the cytotoxicity of several crosslinking agents for chitosan, 3-glycidoxypropyltrimethoxysilane (GPTMS) monomer proved to be less cytotoxic than glutaraldehyde for MG63 human osteosarcoma cells [14]. The chitosan-GPTMS hybrids are degradable with a controllable degradation rate because the crosslinking ratio and formation of a Si-O-Si network. The grafting of Si-OH groups or Si-O-Si networks into the polymer also induces bioactive properties. However, this precursor requires pH neutralization for application in the human body. β-glycerophosphate (β-GP) is a weak base and one of the osteogenic supplements used for the cultures of human bone marrow mesenchymal stem cells. Chenite *et al.* [15] prepared injectable hydrogels using chitosan–β-GP and reported their good cartilage tissue regeneration. Shirosaki *et al.*[16] reported that MG63 cells exhibited good cytocompatibility on chitosan-GPTMS-β-GP hydrogels

compared with the chitosan-β-GP system.

Assessment of the degradation behavior of a biomaterial is essential. The human body presents a diverse range of pH levels. The normal range pH reference of arterial blood is 7.35 to 7.45 [17-19]. In contrast, the pH in the stomach of healthy people in the second and third postprandial period varied from 1.7 to 4.3 [20]. Furthermore, the duodenal pH decreased from 6.1 to 5.4 when a meal is ingested [21].

In the present study, a microfluidic approach was used to synthesize chitosan-siloxane-β-GP hybrid microspheres. Their structural composition was analyzed and the degradation behaviors were examined under several pH conditions; in addition, their stability and elemental release from the microspheres matrix were evaluated. The microspheres also incorporated pelargonidin as drug model and their releasing behavior was tested. Pelargonidin is one of the anthocyanins, which have an on the protection against a myriad of human diseases (prevention of cardiovascular and neuronal diseases, diabetes, etc.) by their antioxidant properties [22,23].

2. Materials and Methods

1. Preparation of chitosan-siloxane hybrid microspheres

Chitosan (high molecular weight, DA>75%, Sigma-Aldrich®) was dissolved in 0.1 M

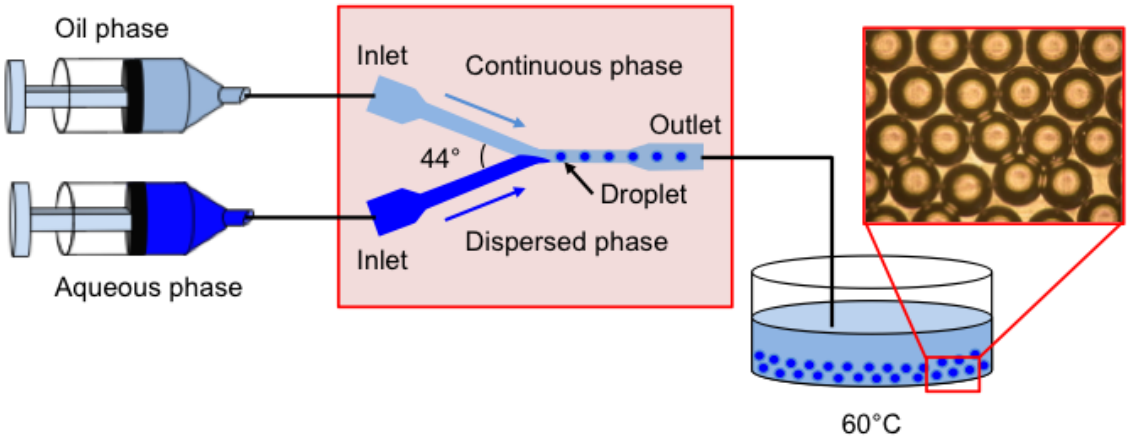

Fig. 1 Schematic representation of the shape and dimensions of the microchannel and microspheres before the gelation.

hydrochloric acid to attain a concentration of 2% (w/v). The chitosan solution was mixed in a planetary centrifugal mixer (ARE-310, Thinky, USA) at room temperature, followed by autoclaving at 121°C for 20 min and filtering (polyethersulfone, 0.22 μm pore) to obtain a homogeneous solution. An appropriate amount of GPTMS (97%, Alfa Aesar) was added to the chitosan solution, and the mixture was stirred at room temperature for 2 h. For 10 mL of chitosan-GPTMS, 3.25 mL of 2.5 M β-GP (pH 9.6, Sigma) was added at 0°C for 10 min to neutralize the precursor sol pH to 7. The microfluidic system consisted of two syringe pumps (YMC KeyChem), one containing the hybrid solution and the other containing the oil solution. Both syringes were connected to a Y-shaped microchannel (Fig. 1). The precursor sol was used as the dispersed phase, and an oily solution of 4% (w/v) span/squalene (Sigma-Aldrich®) was

used as the continuous phase. When both solutions fused in the Y microchannel, the microspheres were formed. The optimized conditions used in the microfluidic system are listed in Table 1. Then the microdrops were gelated at 60°C for 1 h in 4% (w/v) span/squalene oil solution to obtain the wet microspheres. The wet microspheres were rinsed with a series of graded ethanol dilutions (100%, 90%, 80%, 70%, 60%, 50% and 25%) to remove the oil. These microspheres were intended to be used for future biological characterization, therefore the microspheres were sterilized by autoclaving at 121°C for 20 min in distilled water. To incorporate pelargonidin, pelargonidin chloride (Sigma-Aldrich®) was dissolved into 0.1 M HCl and then added into chitosan-GPTMS solution to achieve the concentration of 1 mg/mL. After mixing for 20 min at room temperature, the microspheres with pelargonidin were prepared as following above procedure.

Table 1 Starting compositions of the hybrid microspheres and optimized parameters used in the microfluidic system.

Sample	Molar ratio		Flow rate (mL/min)		Channel (mm)		Outlet (mm)
	Chitosan	GPTMS	Oil	Sol	Depth	Width	
ChG10	1.0	1.0	0.100	0.005	1.0	0.8	1.0
ChG15	1.0	1.5	0.100	0.005	1.0	0.8	1.0

2. Structural characterization of the hybrid microspheres

The size and shapes of the microspheres were examined under a bright-field microscope (IX73, Olympus, Japan). ImageJ v1.48 software (National Institutes of Health, USA) was utilized to measure the diameter of more than 100 microspheres. The surface morphology of the microspheres was examined using SEM (JMS-6010 PLUS/LA, JEOL, Japan) equipped with an energy dispersive X-ray spectrometry (EDS) to detect the elements present in the microspheres at 15 kV operating voltage and a working distance of 10 mm. The samples were coated with a 15 nm thick layer of Pt/Pd using a magnetron-sputter coater (MSP-1S Magnetron Sputter, Vacuum Device Inc., Japan). The surface charge of the microspheres in phosphate buffered saline (PBS, pH7.4, Gibco) and in distilled water were measured via Zeta Potential (ELS-Z, Photal Otsuka Electronics, Japan) using the rectangular cell to determine the surface charge and potential stability. Solid-State ^{13}C, ^{29}Si, ^{31}P, and ^{1}H NMR measurements were performed on an Agilent DDS 500 MHz NMR spectrometer (Agilent Technologies, Inc., Santa Clara, CA, USA) operating at 11.7 Tesla. A zirconia rotor with a diameter of 3.2 mm was used with an Agilent HXY T3-MAS probe. The rotor spinning frequency

for magic angle spinning (MAS) was controlled to be 15 kHz. $^{1}H \rightarrow ^{13}C$ cross-polarization (CP)-MAS NMR experiments were performed with contact time of 500 μs and recycle delay of 10 s, where the signals of 3700 and 5400 pulses were accumulated for ChG15 and ChG10, respectively, with adamantane ($C_{10}H_{16}$) as the external reference (38.52 ppm vs. 0 ppm TMS). In addition, ^{1}H MAS NMR spectra were taken at 499.8 MHz with a 1.15 μs pulse length (pulse angle, π/4) and 5 second recycle delays, where the signals of 8 pulses were accumulated with adamantane ($C_{10}H_{16}$) as the external reference (1.91 ppm vs. 0 ppm TMS). Furthermore, $^{1}H \rightarrow ^{29}Si$ CP-MAS NMR experiments were performed with contact time of 5 ms and recycle delay of 5 s, where the signals of 40580 and 79460 pulses were accumulated for ChG15 and ChG10, respectively, with polydimethylsilane (PDMS) as the external reference (-34.44 ppm vs. 0 ppm TMS). Direct polarization ^{31}P MAS NMR spectra were taken at 202.3 MHz where a 1.4 μs pulse length (π/4-pulse angle) and 120 second recycle delays using $NH_4H_2PO_4$ as the external reference (1.0 ppm vs. 0 ppm 85% H_3PO_4). The signals of 508 and 718 pulses were accumulated for ChG15 and ChG10, respectively. ^{1}H high-power decoupling was used during the ^{31}P acquisition. $^{1}H \rightarrow ^{31}P$ CP-MAS NMR

experiments were also performed with contact time of 1 ms and recycle delay of 5 s, where the signals of 1000 and 2720 pulses were accumulated for ChG15 and ChG10, respectively. Weight measurements were performed before and after drying at 100°C until the microspheres were completely dried. The following equation was used to determine the water content:

$$\text{Water content (\%)} = (Ww - Wd)/Ww \times 100 \qquad \text{Eq. (1)}$$

were, Ww and Wd represent the wet and dry weight, respectively.

3. Compression assay and thermogravimetric analysis

Compression tests (Rheoner II Creep meter RE2-3305C, Yamaden, Japan) were performed to evaluate the stress-deformation behavior of the microspheres under a uniaxial compressive load. A 20 N load was applied using a cylindrical probe with 3 mm of diameter, and a descending speed of 0.05 mm/sec. The compression tests of individual microspheres were performed with replicates for both ChG10 and ChG15. Thermal decomposition of the samples was conducted with simultaneous recording of the weight loss using thermogravimetric analysis (TG) and differential thermal analysis (DTA) (TG-DTA 2000S, Mac Science, Co., Yokohama, Japan) with a heating rate of

10°C/min in air from room temperature to 800°C.

4. Degradation assay under several pH conditions and drug releasing test at acidic condition

The 200 microspheres were incubated in solutions under three different pH conditions. According to the literature, the gastric juices secreted by parietal cells from the stomach consist of 0.1 M HCl [24,25]. Therefore, to mimic the gastric acid conditions, the microspheres were incubated in 0.1 M HCl solutions of pH 1.7 and 5.4 (adjusted with using 0.2 M NaOH) at 36.5°C (water bath) and agitated at 100 rpm for 14 days. For neutral pH condition, the same number of microspheres was incubated in PBS (pH 7.4) under the same conditions. At the designated time points, the surrounding excess soaking solution was removed using a pipette for weight measurements. The mass percentage retained in the microspheres was calculated by comparing the remaining weight with the initial weight using the following equation:

$$\text{Weight loss (\%)} = (Wb - Wa)/Wb \times 100 \qquad \text{Eq. (2)}$$

where, Wb and Wa represent the weights before soaked and after soaking, respectively. The supernatant was reserved for pH measurements (pH meter LAQUAtwin B-712,

Horiba, Japan) and to evaluate the elements released from the microspheres matrix. Assessment of the phosphate and silicon released into the supernatant during the degradation assays was performed using inductively coupled plasma atomic emission spectrometer (ICP-AES; ICPE-9820, Shimadzu, Japan). The surface morphology after the degradation tests was also examined using SEM. To determine the potential changes in the sample crystallinity after degradation, the microspheres were examined by powder X-Ray Diffraction (XRD, MXP3V, Mac Science, Co., Yokohama, Japan) with CuKα radiation. The scanning were performed for the 2θ angle ranging from 5.020° to 40.000° with a step size of 0.020°, a counting time of 1 s, an operating voltage and current of 40 kV and 30 mA, respectively. The microspheres with pelargonidin were soaked in 0.1 M HCl of pH 1.7 at 37°C. Sample solutions with or without the microspheres without pelargonidin were also incubated as control condition. The optical absorbance of the supernatant was recorded with an UV-VIS spectrophotometer (DeNovix, DS-11+, DeNovix Inc.) at the highest peak around 225-230 nm. After measuring, the supernatant was inserted again into the respective tube and continued the releasing test.

5. Statistical analysis

The results were analyzed using one-way analysis of variance (ANOVA) followed by Tukey's test with a significance level of $p<0.05$. The statistical analysis was performed using GraphPad Prism (GraphPad Prism Software version 6, CA, United States).

3. Results and Discussion

3.1 Synthesis of microspheres by microfluidic system and their microstructure

The production of the chitosan and chitosan-β-GP without GPTMS was attempted as control but the microspheres were not obtained due to the slow gelation time. Therefore, GPTMS plays an essential role in the synthesis of the microspheres using the microfluidic system. To size uniformity of microparticle is an important parameter, especially if they are applied as drug carriers. The hybrid microspheres fulfilled the size uniformity requirement, and the obtained size was adequate for gastrointestinal drug delivery because it avoids internalization by gastric cells. Indeed, some researchers [26,27] reported the use of microparticles for gastrointestinal drug delivery with sizes ranging

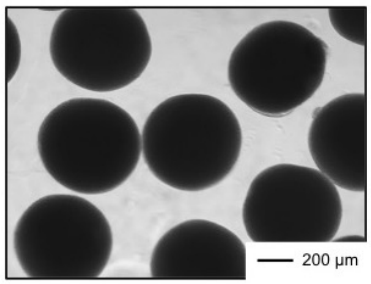

Fig. 2 Brightfield images (obj. 4×) of ChG15 microspheres after gelation.

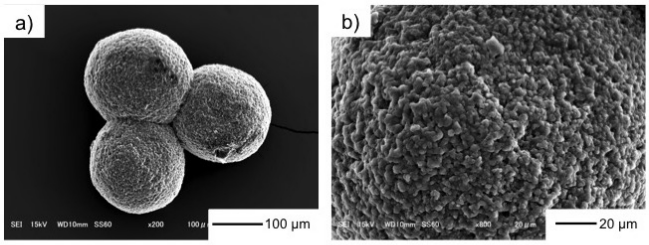

Fig. 3 SEM images of ChG10 dried microspheres before degradation test. b) is a magnified view of a).

from 400-1000 µm with good drug entrapment efficiency. Using the optimized microfluidic conditions reported in Table 1, monodispersed microspheres with uniform size were obtained (Fig. 2), specifically size of 638±15 µm for ChG10 and 661±23 µm for ChG15. In addition, the produced microspheres had a spherical morphology regardless of the molar ratio composition. As observed in previous studies [16], higher GPTMS content resulted in a decrease of the gelation time of the hybrid solution into hydrogels. Consequently, the highest molar ratio used was chitosan:GPTMS=1:1.5; above this ratio, premature gelation of the hybrid solution rapidly occurred in the syringe and microchannel. This gelation led to a higher solution viscosity, which disrupted the flow rate of the solutions, hindering the continuous and long-term production of microspheres. ChG10 and ChG15 contained different amounts of water depending on the GPTMS molar ratio used; for instance, ChG10 contained 87.5% water, whereas ChG15 only contained 59.1% water. The lower water content in the

ChG15 microspheres was expected because of the increase of GPTMS content in ChG15 compared with ChG10. This reduced water content led to higher crosslinking with the chitosan backbone as well as higher condensation of the Si-O-Si network [14], which affected the water content in the matrix of the microspheres. Fig. 3 shows the SEM images of the ChG10 surface. The particles were spherical, even after being dried. Their surface topography was rugged with nanosize pores regardless of the composition. The majority of microscopic materials in contact with a liquid suspension tend to acquire an electronic charge on the material surface [28]. The zeta potential is an indicator of the charge and potential stability of the colloidal system. A greater zeta potential indicates greater stability of the suspension due to the repulsion between charged particles, therefore overcoming the tendency to aggregate that occurs as zeta approaches zero [29]. Ideally, particles with zeta values greater than +30 mV or more negative than -30 mV are considered more stable. However, these values can be affect by the ionic strength and pH, among other factors. Therefore, the zeta potential cannot be considered to exclusively to determine the stability of the system. The hybrid particles presented zeta potential values closer to 30 or -30 mV or half of those values.

In distilled water, ChG10 and ChG15 exhibited zeta potential values of 33.68±1.84 mV and 15.59±2.38 mV, respectively. Whereas, in PBS, ChG10 and ChG15 exhibited values of -13.80±1.49 mV and -27.41±0.92 mV, respectively. Consequently, the surface charge of the hybrid microspheres differed depending on the solution on which they were dispersed suggesting that they tend to interact with ions from the solution. Thus, the negative charge could be due to the interaction of the microspheres with the phosphate ions from PBS. Fig. 4 shows ^{13}C CP-MAS-NMR and ^{31}P DD-MAS-NMR spectra of the ChG10 and ChG15 microspheres. Based on previous study [16], the peaks were assigned to C-1 to C-6, N-acetyl C=O, and N-acetyl-methyl CH_3 signals from chitosan and Cb and Ca from GPTMS. Moreover, two signals of β-GP overlapped with those of C-5,3 and C-6. The presence of Cβ appeared as an increase of the intensity

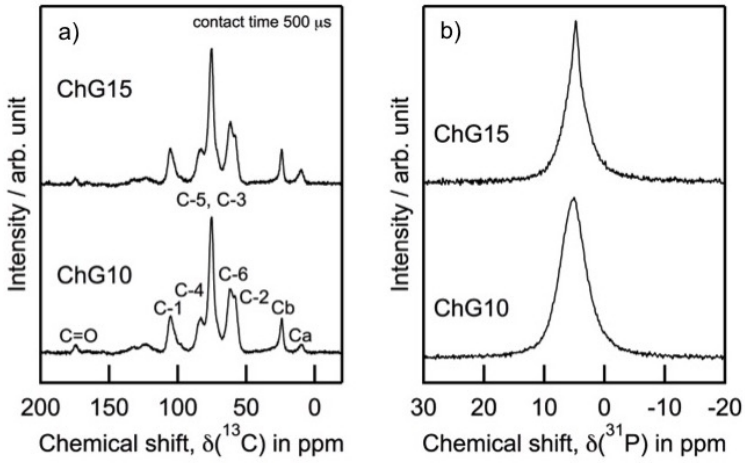

Fig. 4 a) ^{13}C CP-MAS-NMR and b) ^{31}P DD-MAS-NMR spectra of ChG10 and ChG15 microspheres; the corresponding signals are labeled with the chemical structures.

of the C-6 peak. The ^{31}P peaks for the hybrid microspheres were clearly detected at 4.7 ppm for ChG15 and were sharper than those at 5.0 ppm for ChG10. Fig. 5 presents the ^{29}Si CP-MAS-NMR spectra of the ChG10 and ChG15 microspheres. The signals were deconvoluted into four close peaks near -39, -49, -57 and -66 ppm corresponding to the T^0, T^1, T^2 and T^3 species, respectively. The number of Si-O-Si bridging bonds per Si atom represents the degree of polymerization of the -Si-OH or -Si-OR groups at the end of the GPTMS molecules and can therefore be calculated using the following equation:

Degree of polymerization

$$= [(\text{fraction of } T^1) \times 1] + [(\text{fraction of } T^2) \times 2] + [(\text{fraction of } T^3) \times 3] \quad \text{Eq. (3)}$$

The number of Si-O-Si bridging bonds per Si atom derived from the relative peak area of each T^n unit, increased from 2.24 for ChG10 to 2.34 for ChG15, as shown in Table 2. The condensation of GPTMS was accelerated by the amount of GPTMS similar to a previous result [16]. The NMR results indicate the remaining Si-OH is related to water content in the microspheres.

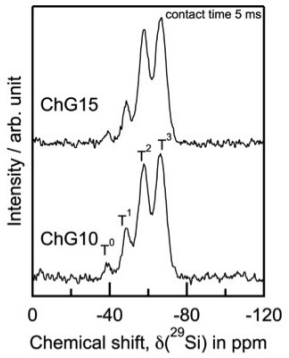

Fig. 5 ^{29}Si CP-MAS-NMR spectra of ChG10 and ChG15 microspheres; the corresponding signals are labeled with the chemical structures.

Table 2 ^{29}Si chemical shifts (δ (ppm)), full width at half maximum (FWHM (ppm)), and relative peak area (I (%)) for T units derived from ^{29}Si CP-MAS NMR spectra.

T unit	T^0			T^1			T^2			T^3			N_{bo}/Si
sample	δ[a]	FWHM[b]	I[c]	δ[a]	FWHM[b]	I[c]	δ[a]	FWHM[b]	I[c]	δ[a]	FWHM[b]	I[c]	
ChG10	-39.1	4.3	3.1	-48.8	5.8	14.7	-57.5	6.2	37.3	-66.4	6.8	44.9	2.24
ChG15	-38.9	3.5	1.9	-48.7	5.1	10.9	-57.6	6.0	38.5	-66.5	6.8	48.7	2.34

[a] The estimated error of the chemical shifts was less than ±0.1 ppm.

[b] The estimated error of the FWHM was less than ±0.2 ppm.

[c] The estimated error of the relative peak area was less than ±0.3%.

3.2 Compressive strength and thermal behavior

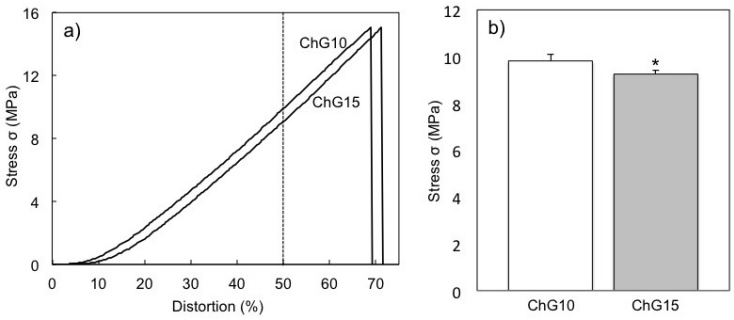

Fig. 6 Compression test results of ChG10 and ChG15 samples. a) ChG10 and ChG15 behavior under uniaxial compression force. b) Stress average of 3 replicates for both microspheres at the same distortion point. * represents a significant difference between ChG10 and ChG15 at the same distortion point ($p<0.05$).

The stress-deformation behaviors of the ChG10 and ChG15 samples are shown in Fig. 6. Repeated tests were performed, and for each condition, the replicates exhibited almost overlapping behaviors. At the maximum elastic-plastic loading, the limit stress of both the ChG10 and ChG15 microspheres was approximately 15 MPa (Fig. 6a) without regaining their original shape. Starting from approximately 20 % distortion, the stress values of the ChG10 samples were slightly higher than those for ChG15.

Therefore, at the 50 % distortion point (Fig. 6b), the averages of the replicates were compared, and a statistical difference was observed between ChG10 and ChG15. This difference could be due to the higher water content and the Si-OH in the matrix of ChG10 microspheres. Fig. 7 shows the TG-DTA curves of the original chitosan flakes, GPTMS monomer, and hybrid microspheres. In general, up to 260°C, a first stage attributed to the vaporization of moisture was observed for all the samples, and all the DTA peaks were exothermic. For the chitosan curve, the weight loss occurred from 251°C to 588°C in two phases after vaporization. The weight loss at each step was 32% and 37%, respectively. Chitosan displayed a very broad and round DTA curve. The first stage was associated with the thermal degradation of the polymeric chain with vaporization of volatile compounds [30]. The pyrolysis of the polysaccharides begins with the fragmentation of the glycosidic links and is associated with weight loss from

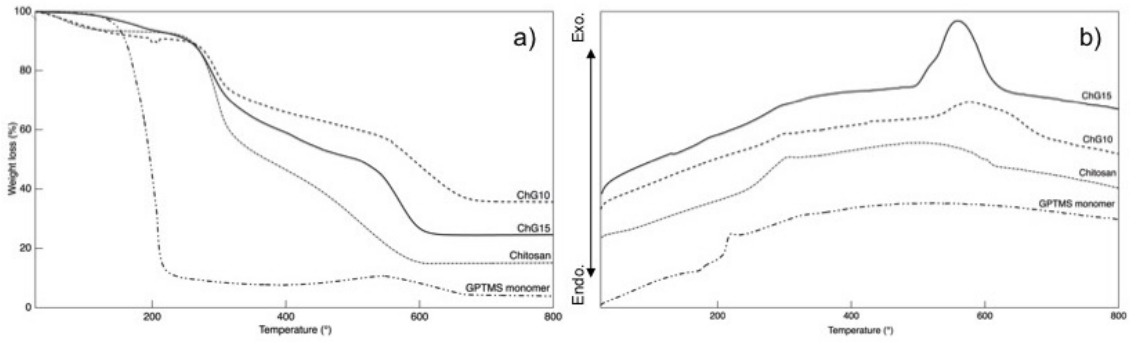

Fig. 7 a) TG and b) DTA curves of chitosan flakes, GPTMS monomer, and ChG10 and ChG15 microspheres.

the non-acetylated and acetylated units of the polymer [31,32]. The second stage of degradation was related to the residual decomposition of chitosan [30,33]. The curve of the GPTMS monomer had a steep slope starting at 159°C until 215°C with a remaining weight of 5%. The steep slope is associated with the degradation of the organic chains of the GPTMS (CH_2 and CH), because the reference boiling point of GPTMS is 120°C (2 mmHg). One additional stage appeared for the weight loss of the microspheres compared with chitosan with the existence of a noticeable DTA curvy peak at 560°C and 580°C. In terms of mass loss, ChG10 lost approximately 13% from 274°C to 316°C, 18% to 554°C with a final slope of 19% mass loss. Similarly, the ChG15 microspheres underwent mass losses of approximately 18% from 261°C to 311°C, 25% to 537°C, and 20% in the final stage.

3.3 Degradability of hybrid microspheres under several pH conditions

Fig. 8a-c shows the weight loss (%) of the hybrid microspheres under 1.7, 5.4 and 7.4 pH conditions. The pH7.4 series exhibited the lowest weight losses of 27% for ChG10 and 32% for ChG15. Although degradation of the microspheres occurred faster in the pH 5.4 and pH 1.7 series, the weight losses of ChG10 of ChG15 were 43% and 59%,

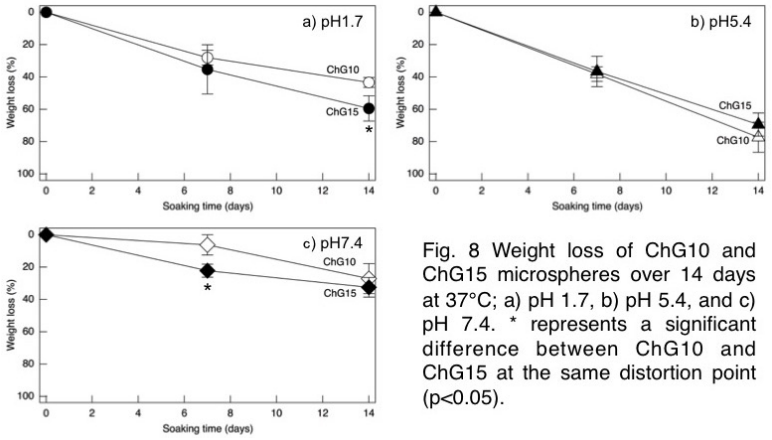

Fig. 8 Weight loss of ChG10 and ChG15 microspheres over 14 days at 37°C; a) pH 1.7, b) pH 5.4, and c) pH 7.4. * represents a significant difference between ChG10 and ChG15 at the same distortion point ($p<0.05$).

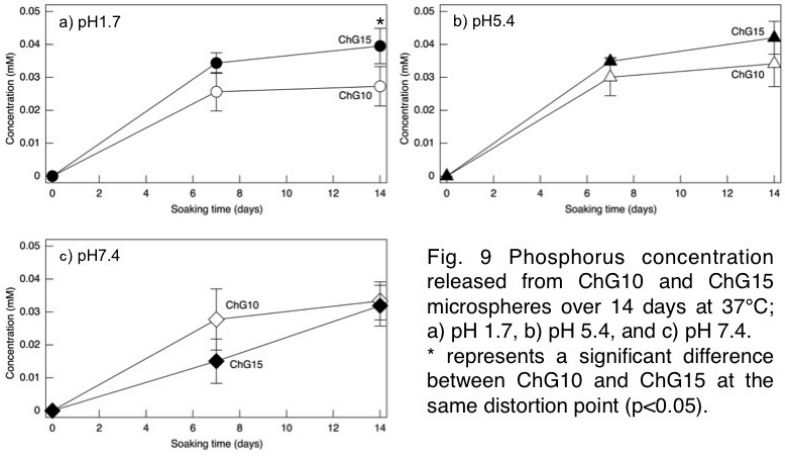

Fig. 9 Phosphorus concentration released from ChG10 and ChG15 microspheres over 14 days at 37°C; a) pH 1.7, b) pH 5.4, and c) pH 7.4. * represents a significant difference between ChG10 and ChG15 at the same distortion point ($p<0.05$).

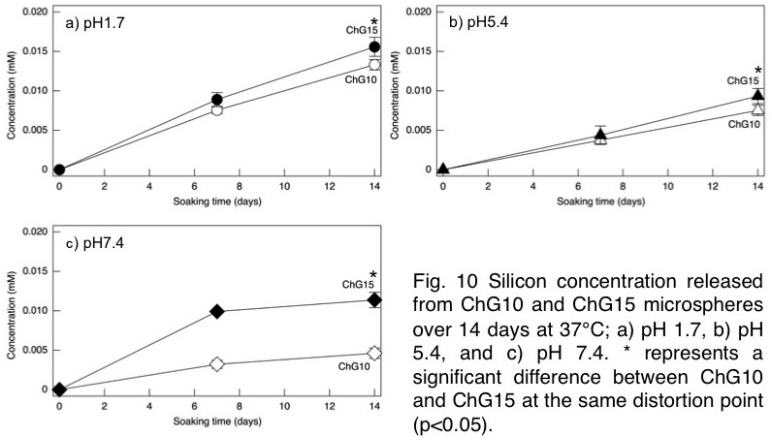

Fig. 10 Silicon concentration released from ChG10 and ChG15 microspheres over 14 days at 37°C; a) pH 1.7, b) pH 5.4, and c) pH 7.4. * represents a significant difference between ChG10 and ChG15 at the same distortion point ($p<0.05$).

respectively, for pH1.7 and 77% and 69%, respectively, for pH5.4. Generally, chitosan can dissolve well in a weak acid near pH 4.5-6.4. However, the chitosan-GPTMS microspheres were gradually degraded and remained after 14 days even at pH 5.7. The

observed weight loss pattern might be beneficial for drug delivery applications (e.g. insoluble drugs, proteins or peptides), because the nutrient adsorption substantially occurs in the duodenum continuing throughout the small intestines [34]. Monitoring the pH helps to understand the degradation and stability of the particles and predict passive or possible harmful effects when they are in contact with living tissues, i.e., a very drastic pH imbalance to acidic conditions can create a detrimental effect.

Table 3 pH values of each solution after soaking the microspheres in the degradation test.

Soaking time (days)	ChG10			ChG15		
	pH 1.7	pH 5.4	pH 7.4	pH 1.7	pH 5.4	pH 7.4
7	1.7±0.0	6.2±0.0	7.3±0.1	1.8±0.1	6.2±0.0	7.3±0.1
14	1.7±0.0	6.4±0.1	7.2±0.1	1.7±0.0	6.4±0.1	7.3±0.1

Table 3 summarizes the pH changes during the 14 days. Under pH 1.7 and 7.4 conditions, both ChG10 and ChG15 were stable with almost no deviation from the initial pH. For pH 5.4, an increase in the pH was observed mostly at 7 days with a final pH after 14 days of 6.4. Fig.9 and Fig.10 show the released amount of phosphorus and silicon from the microspheres in solutions with different pH values. The released amount of phosphorus increased within 14 days. After 14 days, nearly all the samples had released similar amounts of 0.0421 mM regardless of the pH. For the silicon, the

released amount also increased with the soaking time. The ChG15 series released more silicon than the ChG10 series. In addition, more silicon was released at pH 1.7. The phosphate release depended on the composition and the surface charge because of the weak electrostatic chemical interaction between the negatively charged phosphate molecules from β-GP ($-PO_4^{2-}$ or $-HPO_4^-$) and positively charged chitosan ($-NH_3^+$) [33]. The amino groups of ChG15 were crosslinked with GPTMS more than ChG10, preventing the amino groups from interacting with the phosphate groups. Therefore, without interaction with amino groups, the residual β-GP was easily released. The released amount of silicon depends on the crosslinked amount with amino groups because silicon released with chitosan chains. SEM micrographs of the dried

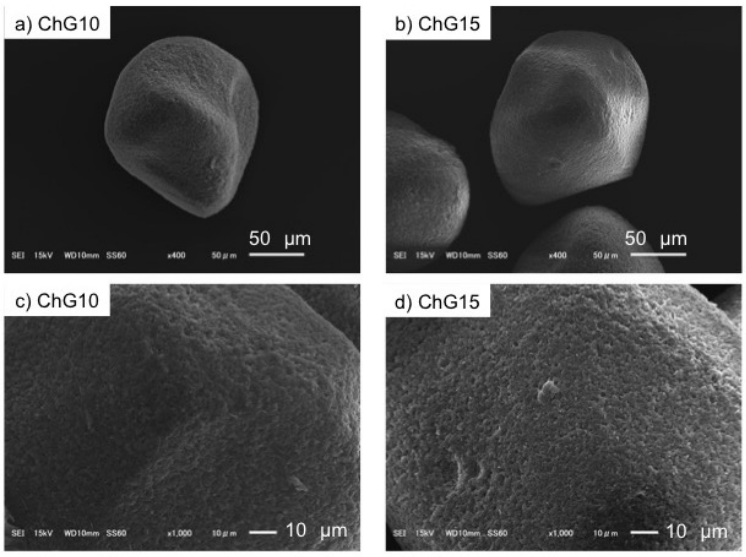

Fig. 11 SEM images of ChG10 and ChG15 dried microspheres after 14 days degradation test at pH 5.4. c) and d) are magnified view of a) and b), respectively.

microspheres after 14 days of degradation at pH 5.4 are presented in Fig.11. After 14 days, there were no dramatic signs of severe surface deterioration for most of the pH conditions, however, the ragged surface became slightly smooth. The spherical shape was only lost for the 5.4 pH series after 14 days because the degradation. The XRD spectra in Fig. 12 confirms the chitosan skeleton degradation with the loss of the peak at 2θ=20° (corresponding to (022) and (102) planes, ICDD #39-1894) for the ChG10 microspheres after 14 days under several pH conditions. However, the pH 7.4 series still showed a very weak peak and was close to becoming amorphous. The degradation results suggested the following degradation steps. (1) β-GP interacted with chitosan released. (2) The chitosan matrix was relaxed, and the solution entered the space, resulting in a reduction of the chitosan crystallinity. (3) Finally, the chitosan molecule was hydrolyzed to form fragments and the crosslinked siloxane units were also released with the chitosan fragments from the microspheres. Therefore the amount of released silicone corresponded to the composition of the microspheres. Moreover, the

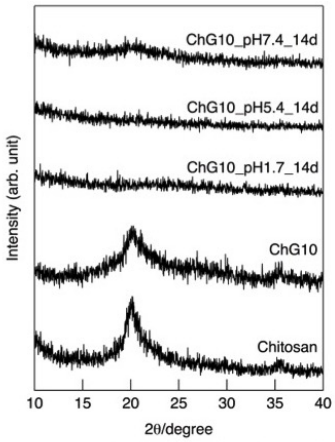

Fig. 12 XRD patterns of chitosan flake, and ChG10 microspheres before and after 14 days degradation test under several pH conditions.

degradation of the microspheres from the surface observed using SEM was confirmed.

For the microspheres to be used as drug delivery systems for the gastrointestinal track, it is important to consider the effects of the chitosan, phosphorus, and silicon released and the limit tolerated by the body without side effects. Considering that chitosan has been approved as a food additive by regulatory entities such as the FDA, the uptake of degradation products from chitosan is considered safe for the body. Phosphorus plays a crucial biological role in the health of bones, and the concentration in serum varies with age; in infants, the normal range is 1.50-2.65 mM, and in adults, the normal range is 0.8-1.5 mM [34]. However, Van Dyck *et al*. [37] stated that the average concentration of silicon in sera in healthy Belgians (including pregnant women) was approximately 4.24 mM. Therefore, the maximum amount of both element released from the hybrid microspheres were very low, suggesting no harmful effect to the human body.

Figure 13 showed the release profile of pelargonidin from ChG15 microspheres within 24 h in SGF. The pelargonidin release occurs mainly within the first 2 hours of incubation. The rapid release within 2h is ascribed to a simple diffusion. After 2 hours, a plateau period was observed. Figure 14 showed images of the samples after 24 hours

incubation. The microspheres are still colored by pelargonidin. The results suggested that the pelargonidin can be released at acidic condition very slowly following the degradation of the microspheres.

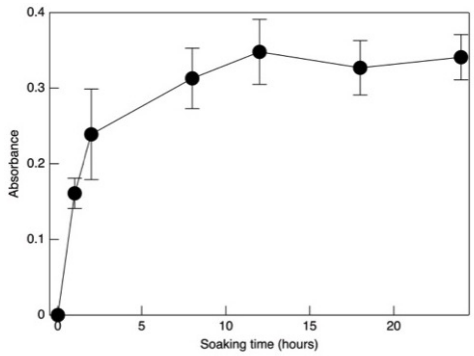

Fig. 13 Releasing profile of pelargonidin from the microspheres (ChG15) in SGF (pH1.7) at 37°C up to 24 hours.

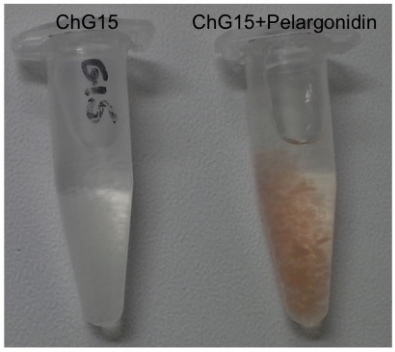

Fig. 14 An image of the microspheres after releasing test for 24 hours.

4. Conclusion

Chitosan-siloxane hybrids microspheres were successfully synthesized using a microfluidic approach via sol–gel process with β-GP as the neutralizing agent. The microspheres had uniform spherical shapes with sizes of approximately 650 μm. Crosslinking with GPTMS inhibited chitosan degradation even at low pH, and the spherical shapes were maintained after 14 days of degradation. Siloxane networks were formed in the chitosan matrix and condensation was promoted by the GPTMS content. Phosphate was easily released because of its weak interaction with chitosan. However, the amount of silicon released with chitosan degradation was dependent on the

composition of GPTMS. These microspheres withstood harsh pH conditions for 14 days, which is longer than the time needed to complete a full digestion cycle. Moreover, the slow drug releasing was expected with the microspheres at acidic condition. Therefore, the result suggests that the synthesized hybrid microspheres are appropriate for use as drug delivery systems for the gastrointestinal track via oral administration.

Acknowledgements

The authors acknowledge the financial support provided from a grant "Promotion and Standardization of the Tenure-Track System (Kojinsenbatsu)" by the Ministry of Education Culture, Sports, Science and Technology (MEXT), the 6th SHISEIDO Female Researcher Science Grant, the MEXT International Students Scholarship, and Sasakawa Research Grant 2015 from the Japan Science Society.

References

1. V.D. Prajapati, G.K. Jani, J.R. Kapadia, Current knowledge on biodegradable microspheres in drug delivery, Expert Opin. Drug Deliv. 12 (2015) 1283-1299.
2. V.R. Sinha, A.K. Singla, S. Wadhawan, R. Kaushik, R. Kumria, K. Bansal, S. Dhawan, Chitosan microspheres as a potential carrier for drugs, Int. J. Pharm. 274 (2004) 1-33.
3. R. Jalil, J.R. Nixon, Biodegradable poly(lactic acid) and poly(lactide-co-glycolide) microcapsules: Problems associated with preparative techniques and release properties, J. Microencapsul. 7 (1990) 297-325.
4. J. Wan, Microfluidic-based synthesis hydrogel particles for cell microencapsulation and cell-based drug delivery, Polymers 4 (2012) 1084-1108.
5. C. Dhand, N. Dwivedi, X. J. Loh, A. N. J. Ying, N. K. Verma, R. W. Beuerman, R. Lakshminarayanan S. Ramakrishna, Methods and strategies for the synthesis of diverse nanoparticles and their applications: a comprehensive overview, RSC Adv. 5 (2015) 105003-105037.

6. M. Liu, Y. Chang, J. Yang, Y. You, R. He, T. Chen, C. Zhou, Functionalized halloysite nanotube by chitosan grafting for drug delivery of curcumin to achieve enhanced anticancer efficacy, J. Mater. Chem. B, 4 (2016) 2253-2263.

7. E. Ye, X. J. Loh, Polymeric Hydrogels and Nanoparticles: A Merging and Emerging Field, Aust. J. Chem. 66:9 (2013), 997-1007.

8. Z. Li, E. Ye, David, R. Lakshminarayanan, X. J. Loh, Recent Advances of Using Hybrid Nanocarriers in Remotely Controlled Therapeutic Delivery, Small 2016, 12:35 (2016) 4782-4806.

9. G. Coue, J.F.J. Engbersen, "Cationic polymers for intracellular delivery of proteins", in Cationic polymers in regenerative medicine, S.K. Samal, P. Dubruel, Eds., pp. 365-367, Royal Soc. Chem. (2014).

10. T. Chandy, C.P. Sharma, Chitosan-as a biomaterial, Biomater. Artif. Cell. Organs 18 (1990) 1-24.

11. E. Khor, L.Y. Lim, Implantable applications of chitin and chitosan, Biomater. 24 (2003) 2339-2349.

12. C. Godugu, A.R. Patel, R. Doddapaneni, J. Somagoni, M. Singh, Approaches to improve the oral bioavailability and effects of novel anticancer drugs berberine and betulinic acid, PLoS ONE 9 (2014) e89919.

13. M. Thanou, J.C. Verhoef, P. Marbach, H.E. Junginger, Intestinal absorption of octreotide: N-trimethyl chitosan chloride (tmc) ameliorates the permeability and absorption properties of the somatostatin analogue in vitro and in vivo, J. Pharm. Sci. 89 (2000) 951-957.

14. Y. Shirosaki, T. Okayama, K. Tsuru, S. Hayakawa, A. Osaka, In vitro bioactivity and MG63 cytocompatibility of chitosan-silicate hybrids, Int. J. Mater. Chem. 3 (2013) 1-7.

15. A. Chenite, C. Chaput, D. Wang, C. Combes, M.D. Buschmann, C.D. Hoemann, J.C. Leroux, B.L. Atkinson, F. Binette, A. Selmani, Novel injectable neutral solutions of chitosan form biodegradable gels in situ, Biomater. 21 (2000) 2155-2161.

16. Y. Shirosaki, M. Hirai, S. Hayakawa, E. Fujii, M.A. Lopes, J.D. Santos, A. Osaka, Preparation and in vitro cytocompatibility of chitosan–siloxane hybrid hydrogels, J. Biomed. Mater. Res. Part A 103 (2015) 289-299.

17. A. Hale, M.J. Hovey, “Acidosis and Alkalosis”, in Fluid, electrolyte, and acid-base imbalances: Content review plus practice questions, pp. 183, F. A. Davis (2013).

18. J. Thomas, W. Klingler, “The influence of pH and other metabolic factors on fascial properties”, in Fascia: The tensional network of the human body: The science and clinical applications in manual and movement therapy, pp. 171, R. Schleip, T.W. Findley, L. Chaitow, P. Huijing, Eds., Elsevier Health Sciences UK (2013).

19. B. Herlihy, “Water, Electrolyte, and Acid-Base Balance”, in The human body in health and illness. pp. 485-488, Elsevier Health Sciences (2014).

20. L. Ovesen, F. Bendtsen, U. Tage-Jensen, N.T. Pedersen, B.R. Gram, S.J. Rune, Intraluminal ph in the stomach, duodenum, and proximal jejunum in normal subjects and patients with exocrine pancreatic insufficiency, Gastroenterol. 90 (1986) 958-962.

21. J.B. Dressman, R.R. Berardi, L.C. Dermentzoglou, T.L. Russell, S.P. Schmaltz, J.L. Barnett, K.M. Jarvenpaa, Upper gastrointestinal (gi) ph in young, healthy men and women, Pharm. Res. 7 (1990) 756-761.

22. B. He, J. Ge, P. Yue, X.Y. Yue, R. Fu, J. Liang, X. Gao, Loading of anthocyanins on chitosan nanoparticles influences anthocyanin degradation in gastrointestinal fluids and stability in a beverage, Food Chem. 221 (2017) 1671-1677.

23. S. Kanokpanont, R. Yamadech, P. Aramwit, Stsbility enhancement of mulberry-extracted anthocyanin using alginate/chitosan microencapsulation for food supplement, Artif. Cells Nanomed. Biotechnol. DOI: 10.1080/21691401.2017.1339050 (2017) .

24. J.G. Cannon, “Peptic ulcer and reflux esophagitis”, in Pharmacology for chemists, pp. 288, Oxford University Press (2007).

25. S. Milan, F. E. Rosato, “Nutrient disposition and response”, in Handbook of drug-nutrient interactions, pp. 120-125, J.I. Boullata, V.T. Armenti, Eds., Humana Press (2010).

26. V. Carelli, S. Coltelli, G. Di Colo, E. Nannipieri, M.F. Serafini, Silicone microspheres for ph-controlled gastrointestinal drug delivery, Int. J. Pharm. 179 (1999) 73-83.

27. S. Khatri, R. Awasthi, Piperine containing floating microspheres: An approach for drug targeting to the upper gastrointestinal tract, Drug Deliv. Transl. Res. 6 (2016) 299-307.

28. L. Mu, S. S. Feng, Fabrication, characterization and in vitro release of paclitaxel (taxol®) loaded poly (lactic-co-glycolic acid) microspheres prepared by spray drying technique with lipid/cholesterol emulsifiers, J. Control. Release 76 (2001) 239-254.

29. R.K. Pujala, "Materials and Characterization Techniques", in Dispersion stability, microstructure and phase transition of anisotropic nanodiscs, pp. 30-31, Springer Theses (2014).

30. F. A. López, A.L.R. Mercê, F.J. Alguacil, A. López-Delgado, A kinetic study on the thermal behaviour of chitosan, J. Therm. Anal. Calorim. 91 (2008) 633-639.

31. J.M. Nieto, C. Peniche-Covas, G. Padron, Characterization of chitosan by pyrolysis-mass spectrometry, thermal analysis and differential scanning calorimetry, Thermochim. Acta 176 (1991) 63-68.

32. C.G.T. Neto, J.A. Giacometti, A.E. Job, F.C. Ferreira, J.L.C. Fonseca, M.R. Pereira, Thermal analysis of chitosan based networks, Carbohydr. Polym. 62 (2005) 97-103.

33. C. Peniche-Covas, M.S. Jiménez, A. Núñez, Characterization of silver-binding chitosan by thermal analysis and electron impact mass spectrometry, Carbohydr. Polym. 9 (1988) 249-256.

34. S.S. Gropper, J.L. Smith, J. L. Groff, "The digestive system: mechanism for nourishing the body", in Advanced nutrition and human metabolism, pp. 33-53, Cengage Learning (2008).

35. J. Cho, M.-C. Heuzey, A. Bégin, P.J. Carreau, Physical gelation of chitosan in the presence of β-glycerophosphate: The effect of temperature, Biomacromol. 6 (2005) 3267-3275.

36. M.G.M.G. Penido, U.S. Alon, Phosphate homeostasis and its role in bone health, Pediatr. Nephrol. 27 (2012) 2039-2048.

37. K. Van Dyck, H. Robberecht, R. Van Cauwenbergh, V. Van Vlaslaer, H. Deelstra, Indication of silicon essentiality in humans, Biol. Trace Elem. Res. 77 (2000) 25-32.

Figure captions

Fig. 1 Schematic representation of the shape and dimensions of the microchannel and microspheres before the gelation.

Fig. 2 Brightfield images (obj. 4×) of ChG15 microspehres after gelation.

Fig. 3 SEM images of ChG10 dried microspheres before degradation test. b) is a magnified view of a).

Fig. 4 a) ^{13}C CP-MAS-NMR and b) ^{31}P DD-MAS-NMR spectra of ChG10 and ChG15 microspheres; the corresponding signals are labeled with the chemical structures.

Fig. 5 ^{29}Si CP-MAS-NMR spectra of ChG10 and ChG15 microspheres; the corresponding signals are labeled with the chemical structures.

Fig. 6 Compression test results of ChG10 and ChG15 samples. a) ChG10 and ChG15 behavior under uniaxial compression force. b) Stress average of 3 replicates for both microspheres at the same distortion point. * represents a significant difference between ChG10 and ChG15 at the same distortion point ($p<0.05$).

Fig. 7 a) TG and b) DTA curves of chitosan flakes, GPTMS monomer, and ChG10 and ChG15 microspheres.

Fig. 8 Weight loss of ChG10 and ChG15 microspheres over 14 days at 37°C; a) pH 1.7, b) pH 5.4, and c) pH 7.4. * represents a significant difference between ChG10 and ChG15 at the same distortion point ($p<0.05$).

Fig. 9 Phosphorus concentration released from ChG10 and ChG15 microspheres over 14 days at 37°C; a) pH 1.7, b) pH 5.4, and c) pH 7.4. * represents a significant difference between ChG10 and ChG15 at the same distortion point ($p<0.05$).

Fig. 10 Silicon concentration released from ChG10 and ChG15 microspheres over 14 days at 37°C; a) pH 1.7, b) pH 5.4, and c) pH 7.4. * represents a significant difference between ChG10 and ChG15 at the same distortion point ($p<0.05$).

Fig. 11 SEM images of ChG10 and ChG15 dried microspheres after 14 days degradation test at pH 5.4. c) and d) are magnified view of a) and b), respectively.

Fig. 12 XRD patterns of chitosan flake, and ChG10 microspheres before and after 14 days degradation test under several pH conditions.

Fig. 13 Releasing profile of pelargonidin from the microspheres (ChG15) in SGF (pH1.7) at 37°C up to 24 hours.

Fig. 14 An image of the microspheres after releasing test of 24 hours.

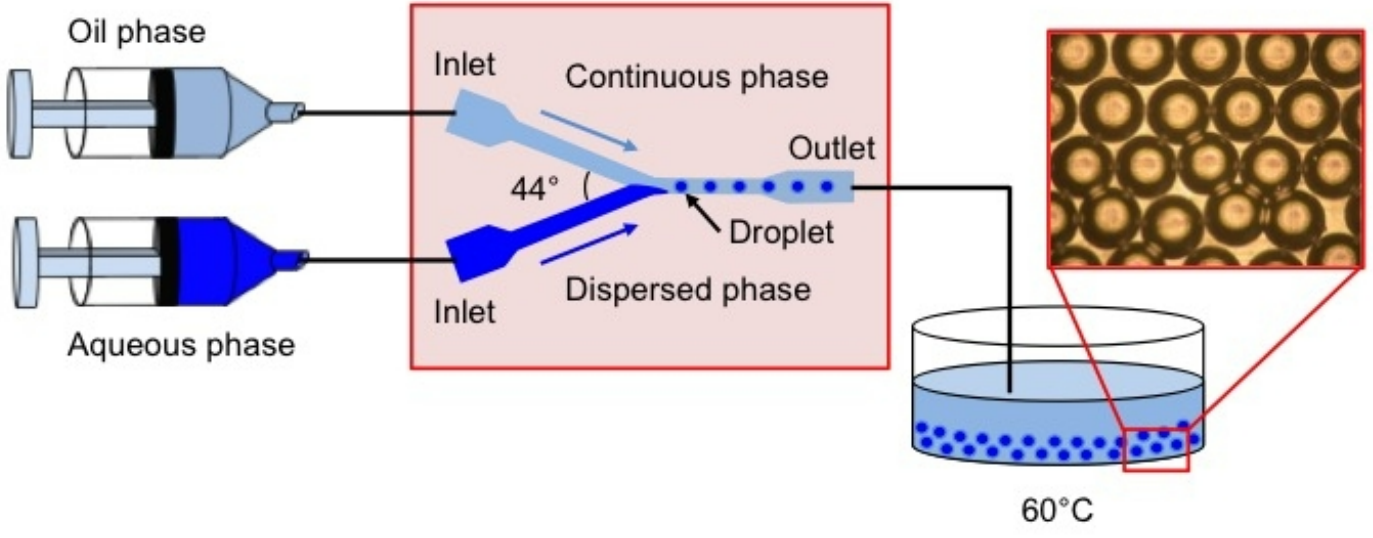

Fig. 1 Neves *et al.*

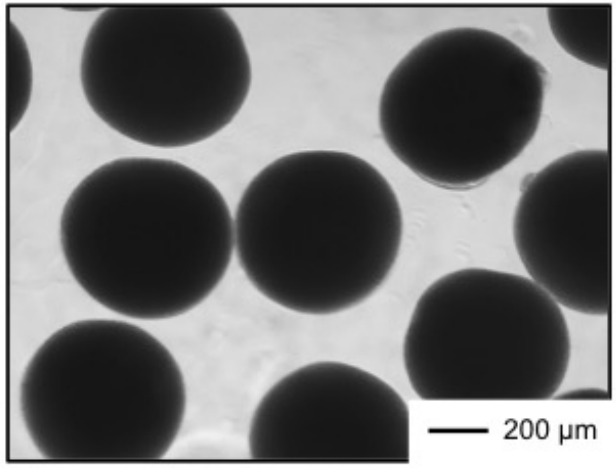

Fig. 2

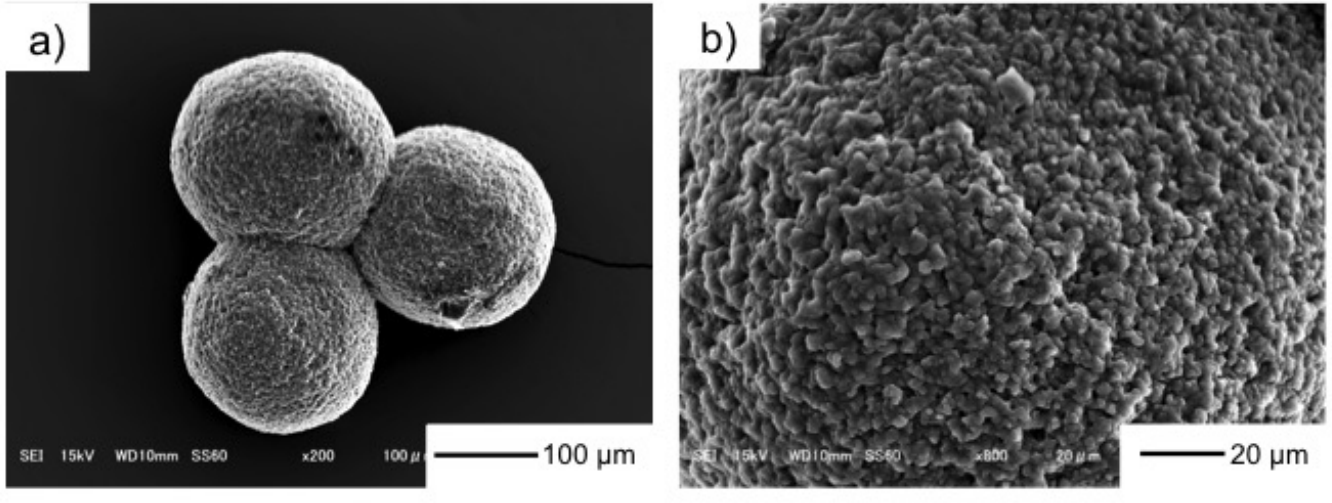

Fig. 3

Neves *et al.*

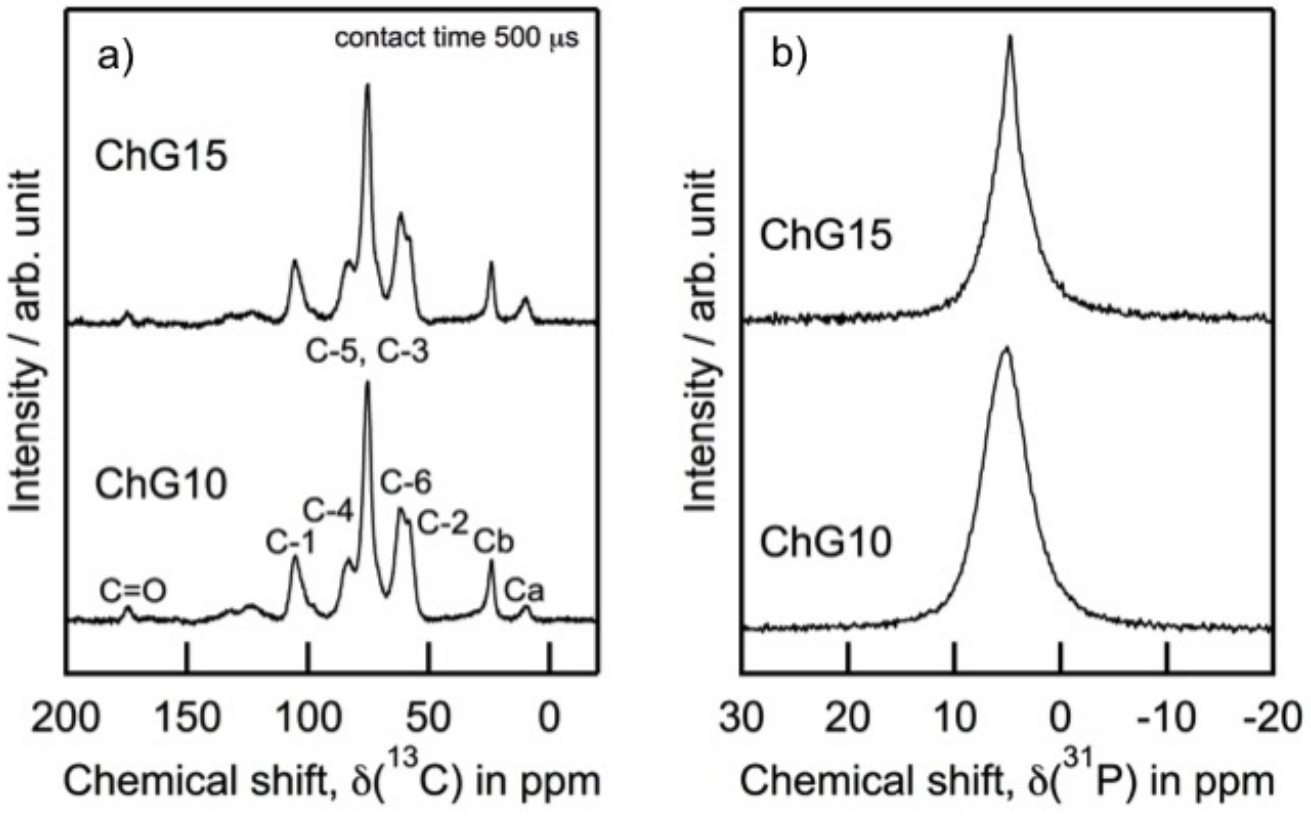

Fig. 4

Neves *et al.*

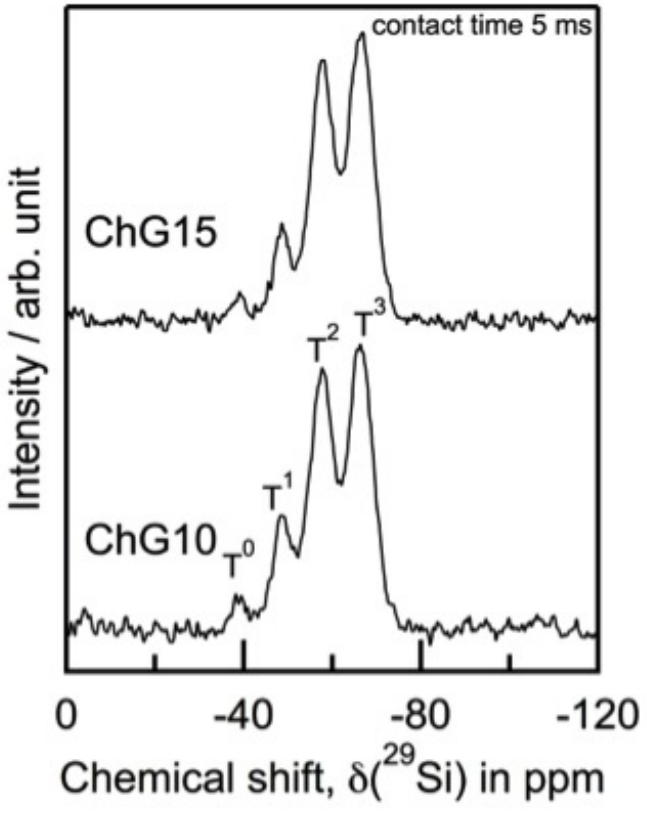

Fig. 5

Neves *et al.*

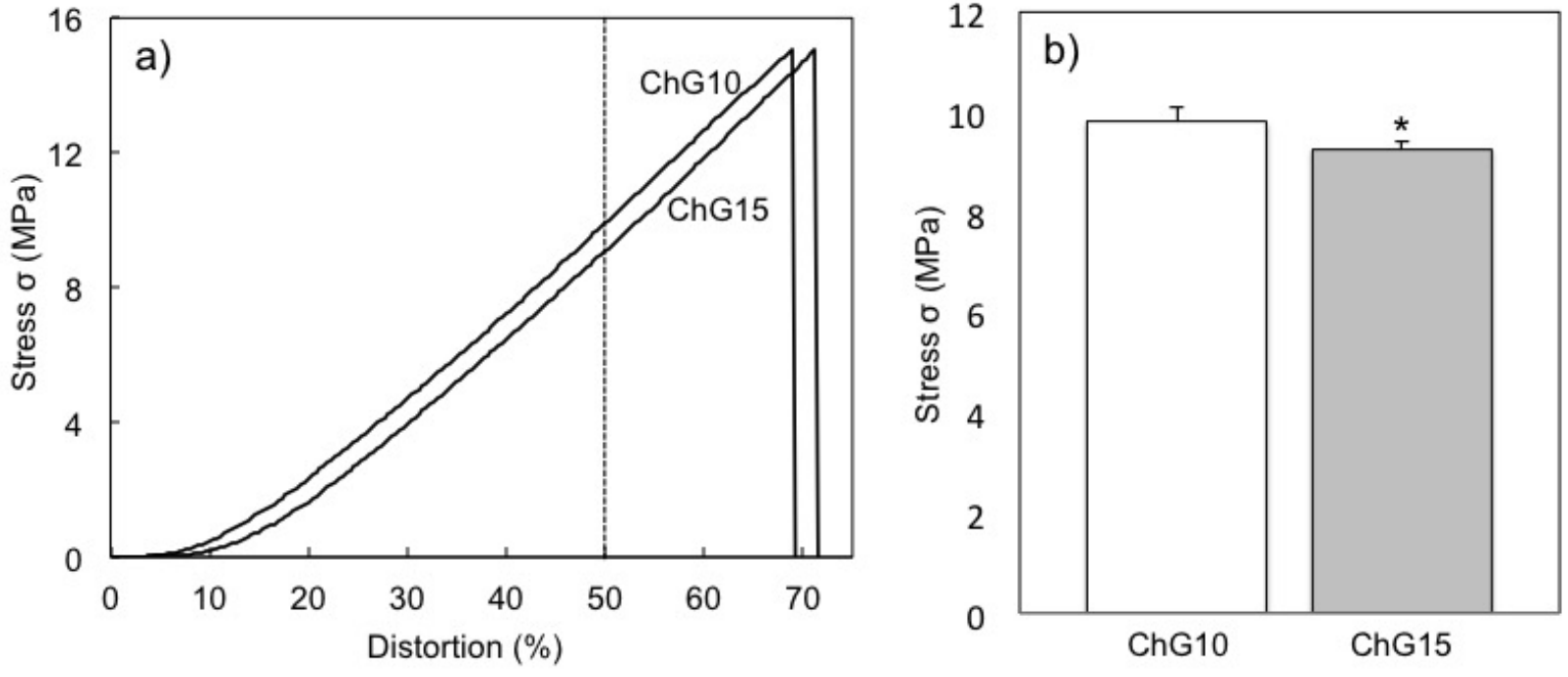

Fig. 6

Neves *et al.*

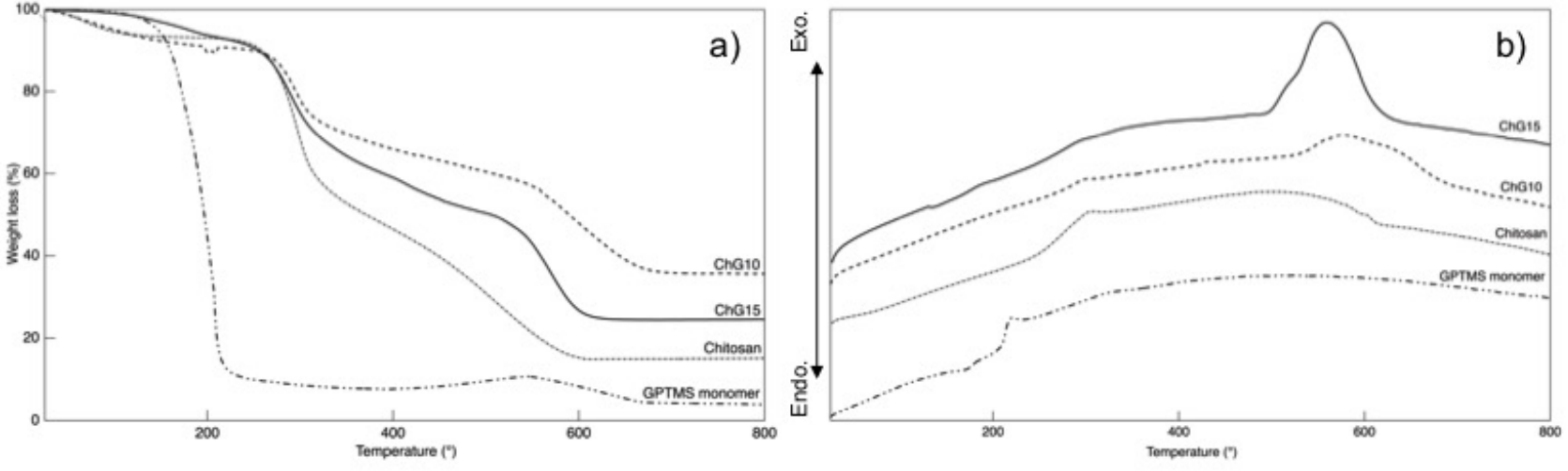

Fig. 7

Neves *et al.*

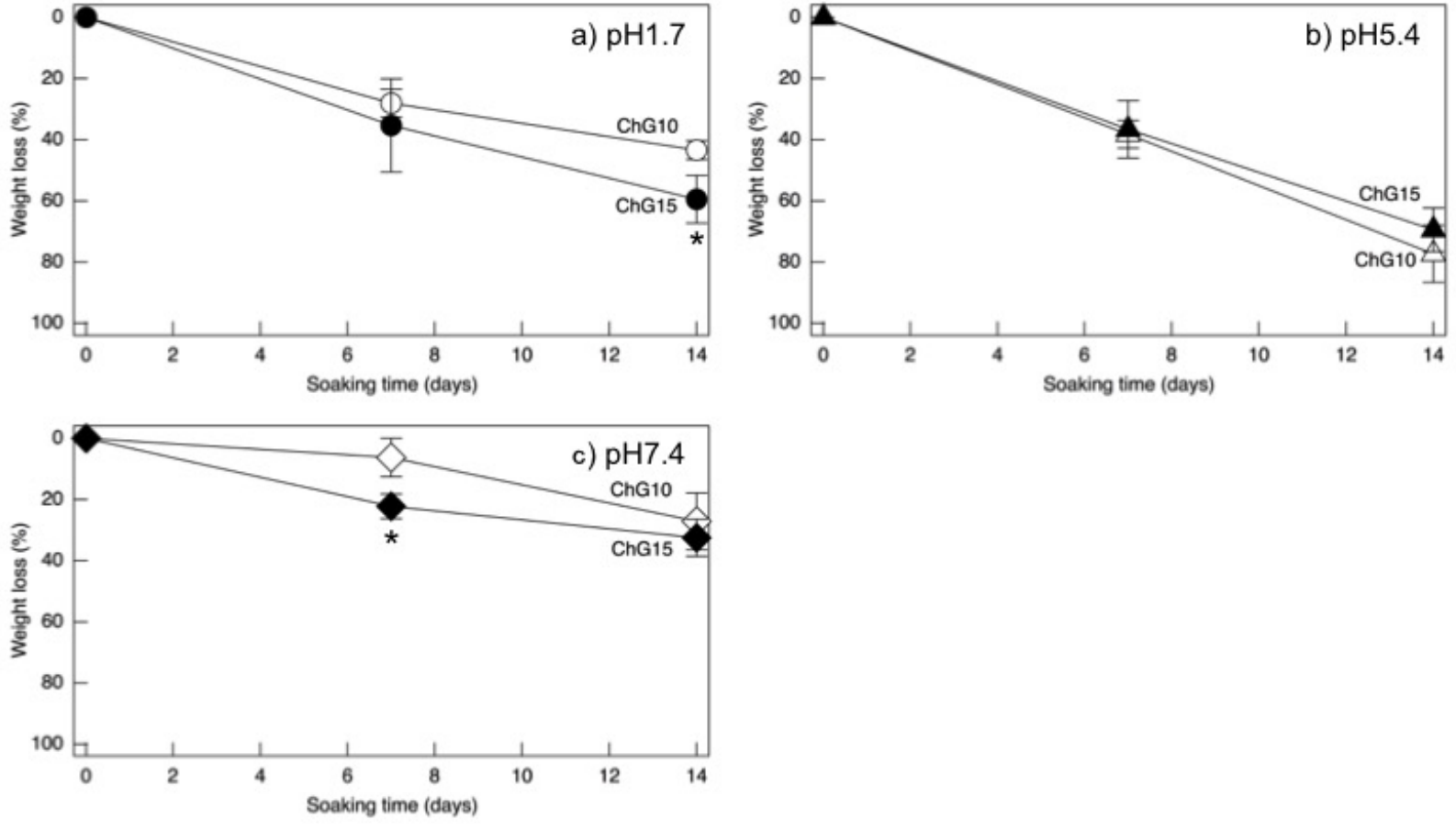

Fig. 8

Neves *et al.*

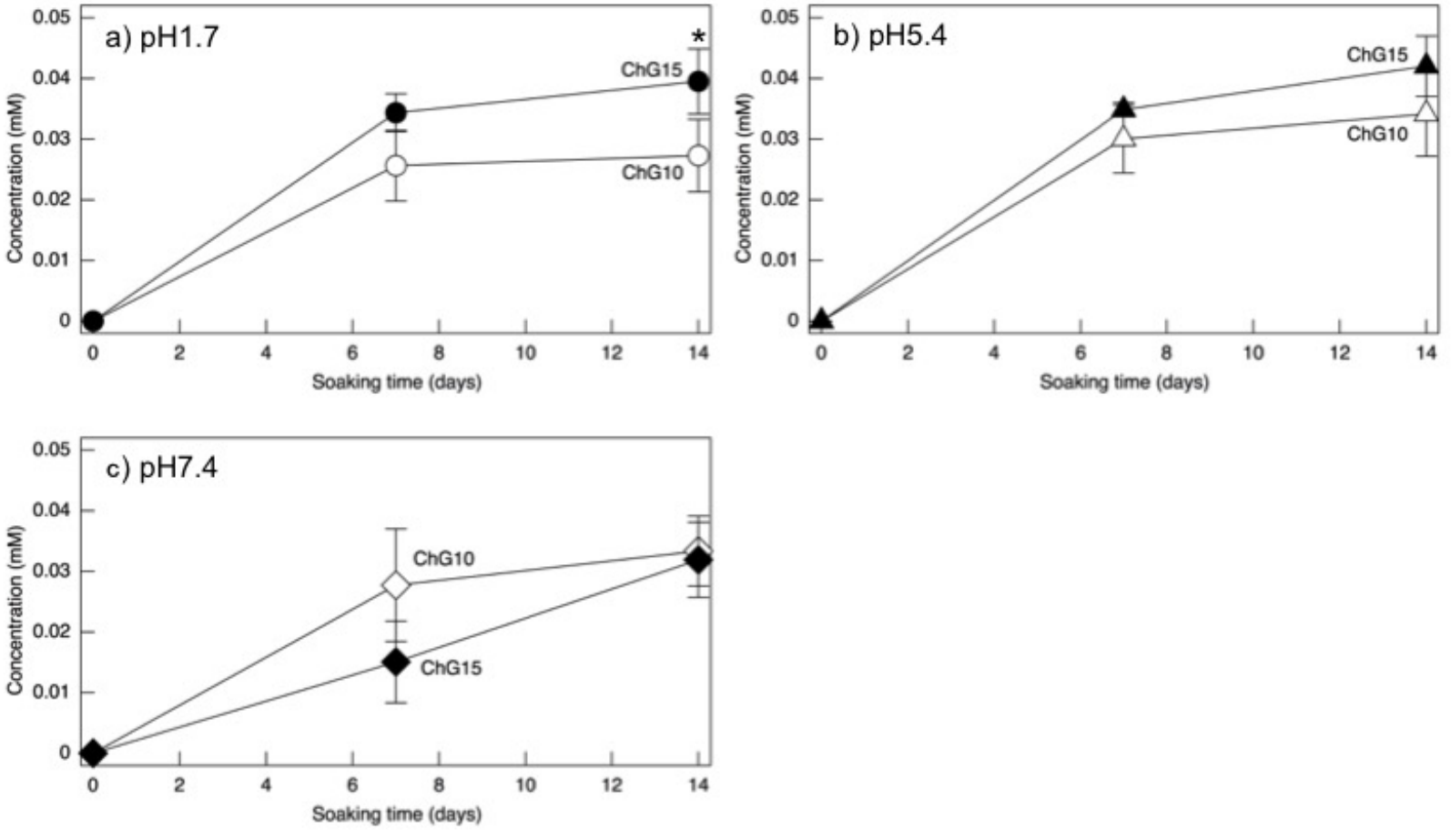

Fig. 9

Neves *et al.*

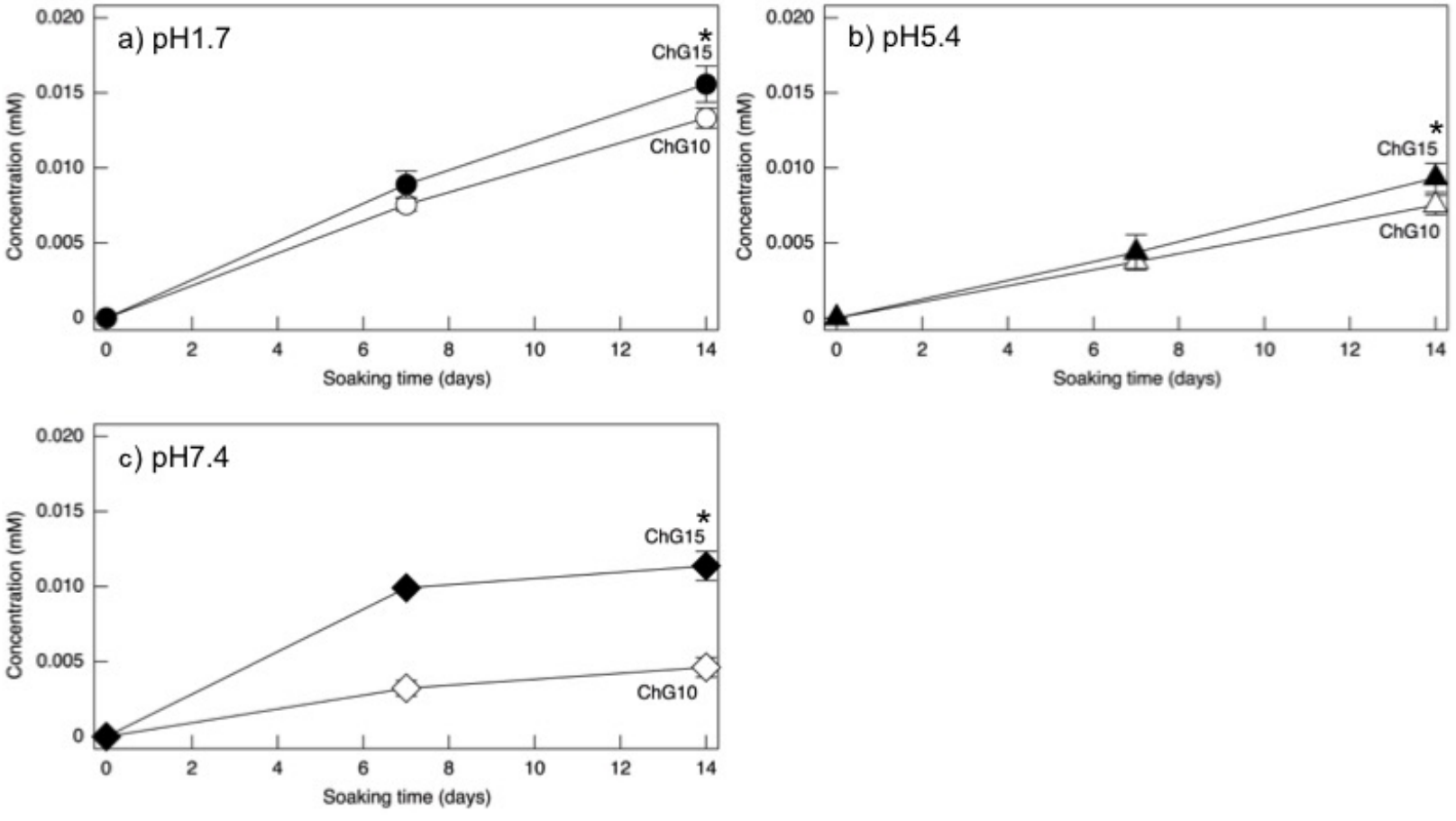

Fig. 10

Neves *et al.*

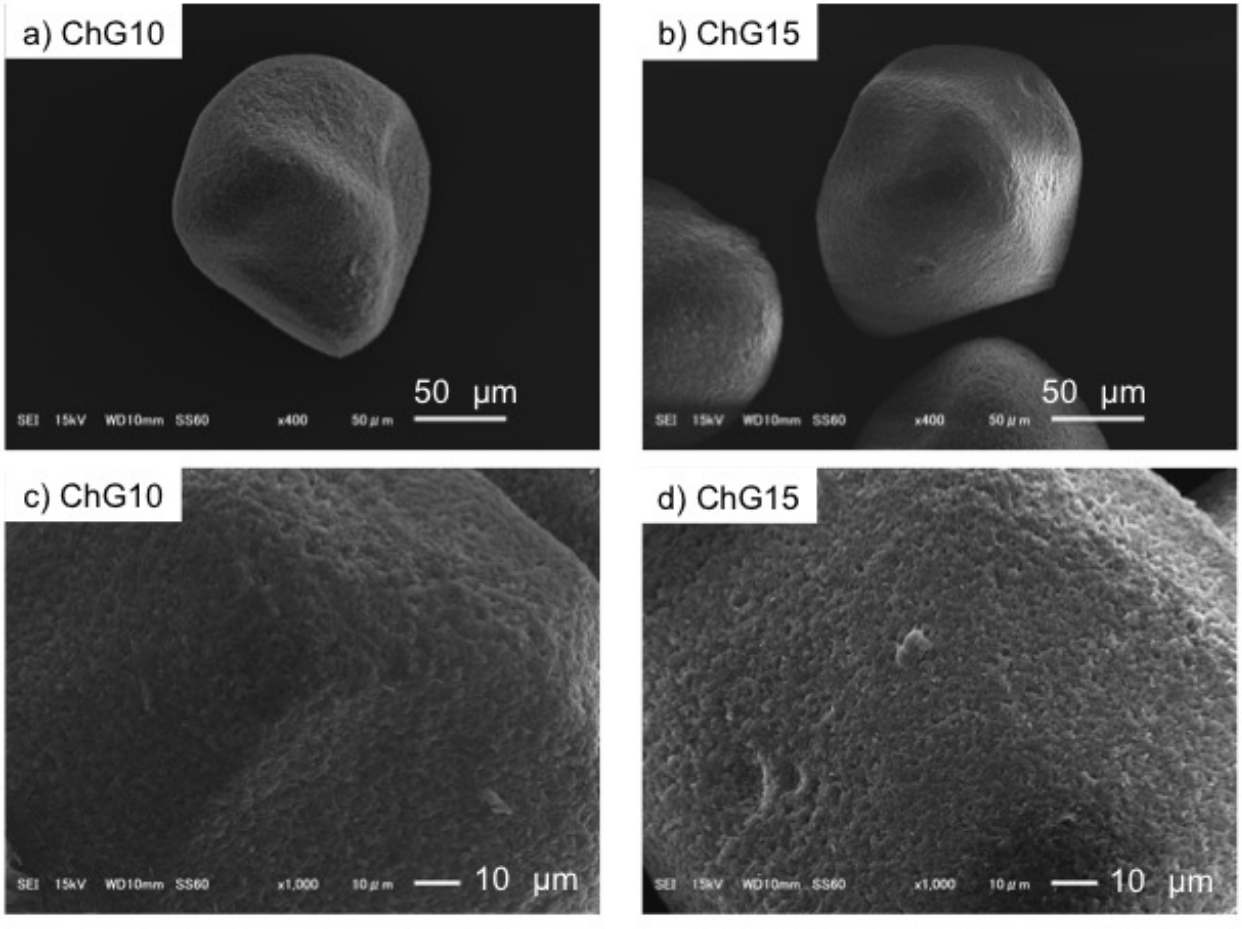

Fig. 11

Neves *et al.*

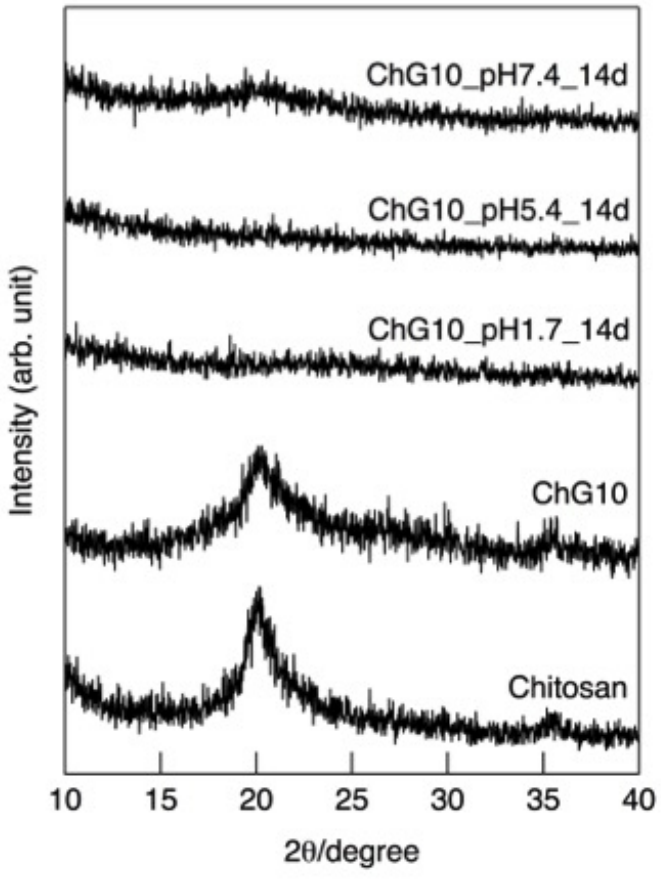

Fig. 12

Neves *et al.*

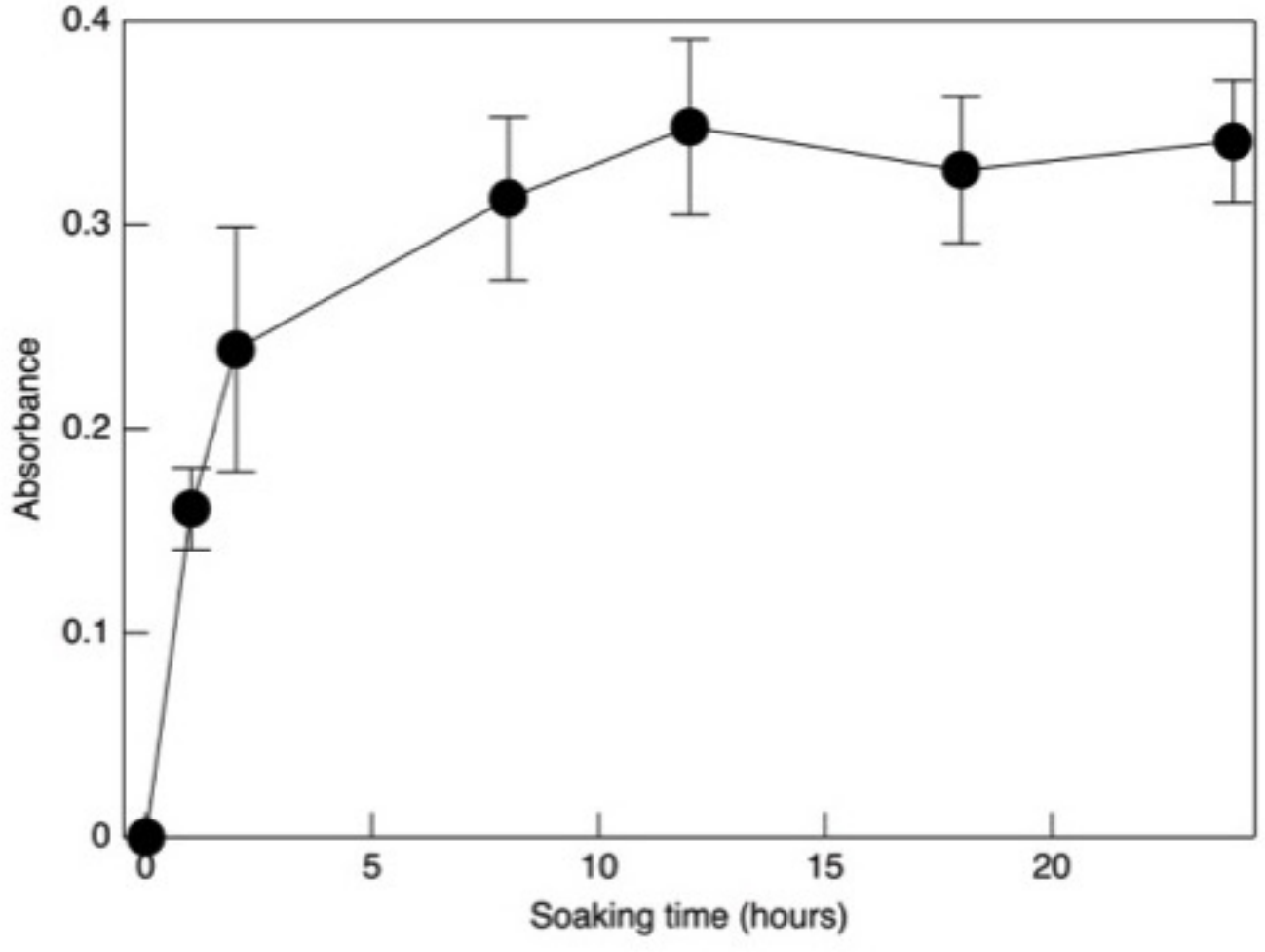

Fig. 13 Releasing profile of pelargonidin from the microspheres (ChG15) in SGF (pH1.7) at 37°C up to 24 hours.

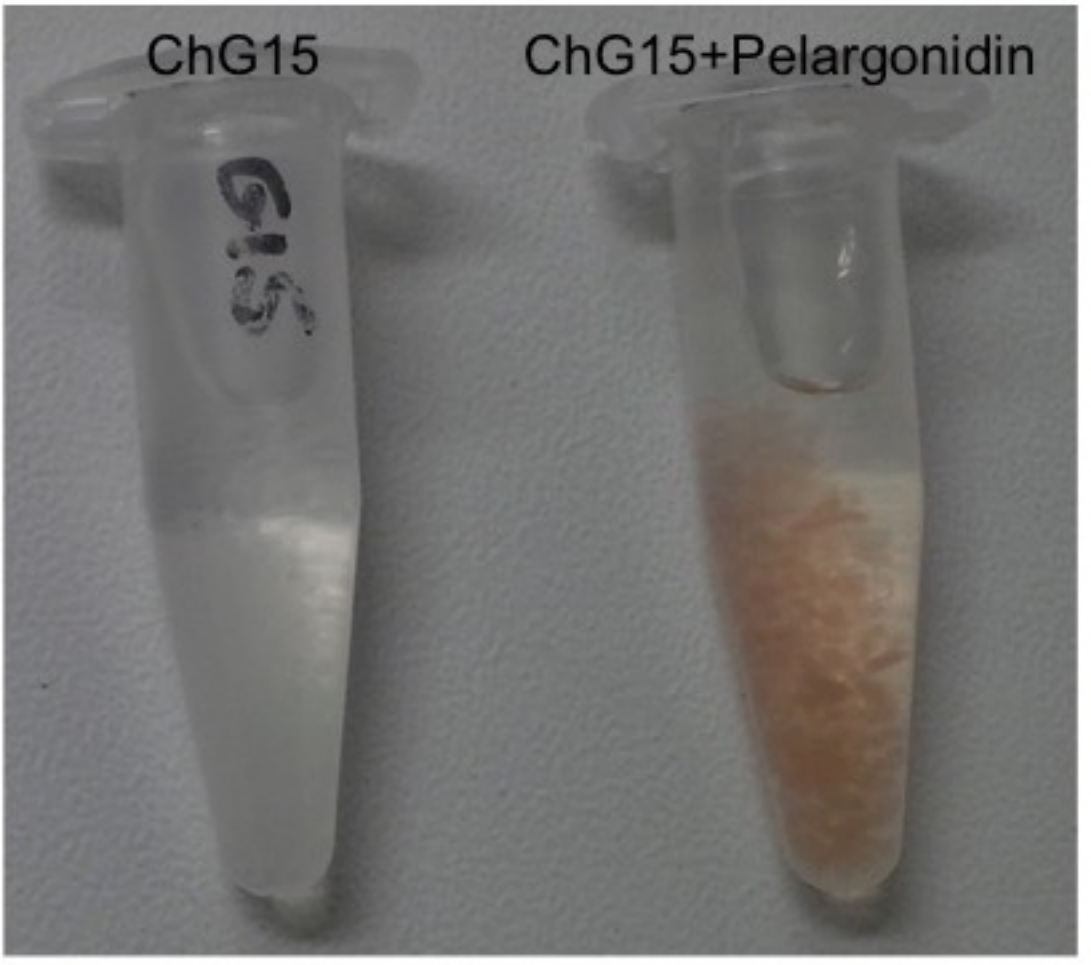

Fig. 14 An image of the microspheres after releasing test for 24 hours.

Table 1 Starting compositions of the hybrid microspheres and optimized parameters used in the microfluidic system.

Sample	Molar ratio		Flow rate (mL/min)		Channel (mm)		Outlet (mm)
	Chitosan	GPTMS	Oil	Sol	Depth	Width	
ChG10	1.0	1.0	0.100	0.005	1.0	0.8	1.0
ChG15	1.0	1.5	0.100	0.005	1.0	0.8	1.0

Table 2 ^{29}Si chemical shifts (δ (ppm)), full width at half maximum (FWHM (ppm)), and relative peak area (I (%)) for T units derived from ^{29}Si CP-MAS NMR spectra.

T unit	T^0			T^1			T^2			T^3			N_{bo}/Si
sample	δ[a]	FWHM[b]	I[c]	δ[a]	FWHM[b]	I[c]	δ[a]	FWHM[b]	I[c]	δ[a]	FWHM[b]	I[c]	
ChG10	-39.1	4.3	3.1	-48.8	5.8	14.7	-57.5	6.2	37.3	-66.4	6.8	44.9	2.24
ChG15	-38.9	3.5	1.9	-48.7	5.1	10.9	-57.6	6.0	38.5	-66.5	6.8	48.7	2.34

[a] The estimated error of the chemical shifts was less than ±0.1 ppm.

[b] The estimated error of the FWHM was less than ±0.2 ppm.

[c] The estimated error of the relative peak area was less than ±0.3%.

Table 3 pH values of each solution after soaking the microspheres in the degradation test.

Soaking time (days)	ChG10			ChG15		
	pH 1.7	pH 5.4	pH 7.4	pH 1.7	pH 5.4	pH 7.4
7	1.7±0.0	6.2±0.0	7.3±0.1	1.8±0.1	6.2±0.0	7.3±0.1
14	1.7±0.0	6.4±0.1	7.2±0.1	1.7±0.0	6.4±0.1	7.3±0.1